Voltage-induced conversion of helical to uniform nuclear spin polarization in a quantum wire

Viktoriia Kornich,[1] Peter Stano,[2] Alexander A. Zyuzin,[1] and Daniel Loss[1,2]
[1]*Department of Physics, University of Basel, Klingelbergstrasse 82, CH-4056 Basel, Switzerland*
[2]*RIKEN Center for Emergent Matter Science, 2-1 Hirosawa, Wako, Saitama 351-0198, Japan*
(Received 29 March 2015; revised manuscript received 28 April 2015; published 18 May 2015)

We study the effect of bias voltage on the nuclear spin polarization of a ballistic wire, which contains electrons and nuclei interacting via hyperfine interaction. In equilibrium, the localized nuclear spins are helically polarized due to the electron-mediated Ruderman-Kittel-Kasuya-Yosida (RKKY) interaction. Focusing here on nonequilibrium, we find that an applied bias voltage induces a uniform polarization, from both helically polarized and unpolarized spins available for spin flips. Once a macroscopic uniform polarization in the nuclei is established, the nuclear spin helix rotates with frequency proportional to the uniform polarization. The uniform nuclear spin polarization monotonically increases as a function of both voltage and temperature, reflecting a thermal activation behavior. Our predictions offer specific ways to test experimentally the presence of a nuclear spin helix polarization in semiconducting quantum wires.

DOI: 10.1103/PhysRevB.91.195423 PACS number(s): 62.23.Hj, 75.75.−c, 73.21.−b, 31.30.Gs

I. INTRODUCTION

Magnetic structures are promising platforms for many modern devices, e.g. memory [1], sensors [2], and quantum computation hardware [3]. The opportunities to get an ordered magnetic phase in the bulk and low-dimensional systems due to Ruderman-Kittel-Kasuya-Yosida (RKKY) interaction [4–7] were studied in a number of theoretical and experimental works [8–13]. The prominent feature of RKKY interaction in one-dimensional (1D) systems is the ordering of localized spins into a helix [14,15].

When the current is driven through the system of electrons and nuclei, the spin polarization can be swapped between the two subsystems through the hyperfine interaction, leading to dynamic nuclear polarization effects [16–21]. If the polarization of current-carrying electrons and localized spins differ, the spin-transfer torque arises [22,23], important for dynamics of domain walls [24,25] and enhancing the tilting of the spiral structure in helimagnets [26]. Closely related is the dynamic nuclear polarization, arising, e.g., in helical edge states of topological insulator. The backscattering of helical electrons can be of different origins, such as assisted by phonons [27], magnetic impurities [28], or absence of axial spin symmetry [29]. It was shown that nuclear-assisted backscattering of electrons due to hyperfine interaction induces nuclear polarization when the current is driven through the edge states of topological insulator [30,31].

The main motivation for our work comes from the recent experiment by Scheller *et al.* [32], where the conductance of a cleaved edge overgrowth GaAs quantum wire was measured. The measurements showed that the conductance of the first mode becomes e^2/h at low temperatures instead of the naively expected $2e^2/h$. This suggests the lifting of electron spin degeneracy. The possible explanation is the presence of a helical nuclear spin polarization that gaps out one subband and thus provides an electron spin selection. Further ways to confirm the presence of the nuclear spin helix were suggested theoretically, by means of nuclear magnetic resonance [33], nuclear spin relaxation [34], and quantum Hall effect anisotropies [35].

In this work, we propose and study a complementary method to detect nuclear spin helical polarization in the wire. It is based on the effect of bias voltage applied to the wire and therefore straightforward to perform experimentally. We investigate how the bias voltage applied to the wire affects its nuclear spin polarization. We assume that at zero bias and finite temperature, nuclear spins are partially polarized into a helix due to the RKKY interaction. We find that an applied voltage induces a uniform nuclear polarization from both helical and nonpolarized nuclear spins available for nuclear spin flips via electrons. Therefore, upon increasing the voltage the helical nuclear polarization drops, while the uniform polarization grows, and the total polarization grows too. For small voltages and increasing temperature, the uniform polarization grows because of thermal activation of electrons, while the helical polarization dramatically drops in magnitude. Once a macroscopic uniform polarization has developed, the remaining nuclear spin helix rotates as a whole around the axis along the uniform polarization. Since the helical polarization affects the conductance of such systems [14,15,32,35], these predicted features are expected to show up in the voltage and temperature dependence of the transport current and thus they can be tested experimentally. Recently, cantilever-based magnetic sensing techniques have been reported which enable nuclear spin magnetometry of nanoscale objects such as the nanowires considered here [36,37]. Such powerful techniques offer promising perspectives for direct experimental tests of the results obtained in this work.

The paper is organized as follows. In Sec. II, we present the Hamiltonian of our model. In Sec. III, we describe the properties of the electron bath. The derivation of the Bloch equation for the total nuclear spin in the wire is discussed in Sec. IV. The resulting nuclear spin polarization and its dependence on the parameters of the system are presented and discussed in Sec. V. Our conclusions follow in Sec. VI. Additional information about our calculation is given in the Appendix.

II. MODEL

We consider a one-dimensional electron gas and localized spins in a semiconductor nanowire. We will refer to these localized spins as nuclear spins in the following, however,

they can be also of other origins, such as, e.g., magnetic impurities, etc. The electrons and nuclei interact via the hyperfine interaction described by the Hamiltonian

$$H_{\rm hyp} = \tfrac{1}{2} A \rho_0^{-1} |\psi_\perp(\boldsymbol{R}_\perp)|^2 \delta(r - R) \boldsymbol{\sigma} \cdot \boldsymbol{I}, \tag{1}$$

where A is a hyperfine constant of the material, ρ_0 is the nuclear spin density, $\psi_\perp$ is the transverse part of electron wave function, r denotes the electron position along the wire, $(R, \boldsymbol{R}_\perp)$ is the position of the nucleus along the wire and in the transverse direction, respectively, $\boldsymbol{\sigma}$ is an electron spin operator, and $\boldsymbol{I}$ is a nuclear spin operator (in units of $\hbar$) with the magnitude I. We assume that the transverse part of the electron wave function $\psi_\perp(\boldsymbol{R}_\perp)$ is constant in the wire cross section, $|\psi_\perp(\boldsymbol{R}_\perp)|^2 = 1/C$, where C is the wire cross-section area. We parametrize it alternatively by the number of nuclear spins in the cross section $N_\perp = Ca\rho_0$, with a being the lattice constant. In GaAs, $\rho_0 = 8/a^3$, $a = 0.565$ nm, $A = 90$ μeV, $I = \frac{3}{2}$, and $N_\perp$ is typically of the order of 10^3. Finally, we introduce $N = L/a$ with L the wire length (typically of order microns), which gives $NN_\perp$ as the total number of nuclear spins in the wire.

We note that in the case where the "wire" is not physically separated from the surrounding medium, the extent of the electronic wave function (confined, e.g., electrostatically) in the transverse direction sets the diameter of the wire in our model. In such a case, we assume that the localized spins, if present outside the wire volume, are not ordered, meaning the surrounding medium is a paramagnet. Such an environment would provide an additional dissipation channel, but would not change the wire spin order, and thus our conclusions, in any qualitative way.

The total Hamiltonian reads as

$$H_{\rm tot} = -\frac{\hbar^2}{2m}\partial_r^2 + H_{\rm hyp}, \tag{2}$$

where m is electron effective mass and $\hbar$ is the Planck constant. If the hyperfine interaction [Eq. (1)] is weak on the energy scale of the electrons, its effects can be treated perturbatively. The condition is quantified by $A \ll \varepsilon_F$, where ε_F is the Fermi energy of the electron system. This condition is well satisfied in the cases we consider here. A Schrieffer-Wolff transformation on $H_{\rm tot}$ perturbatively in $H_{\rm hyp}$, i.e., in order A/ε_F, results to leading order in an effective interaction between the localized spins, the RKKY interaction [4–7,10,11]

$$H_{\rm RKKY} = \sum_{i,j} \boldsymbol{I}_i \cdot J_{ij} \boldsymbol{I}_j. \tag{3}$$

Here, the indexes i, j label the nuclear spins and the RKKY coupling $J_{ij} = J(|R_i - R_j|)$ is related to the static spin susceptibility of electrons (see Eq. (C1) and below in Ref. [35]), giving rise to the spatially dependent RKKY interaction.

Let us rewrite Eq. (3) in the momentum representation, defined through the Fourier transforms $J_q = \sum_{R_i} \exp[-iq(R_i - R_j)]J_{ij}$, with $R_i \in a, 2a, \ldots, Na$, and $\boldsymbol{I}_q = \sum_i \exp(iqR_i)\boldsymbol{I}_i$, with $i \in 1, \ldots, NN_\perp$, and in both cases $q \in (2\pi/N) \times \{0, 1, \ldots, N-1\}$. We get

$$H_{\rm RKKY} = \frac{1}{N} \sum_q \boldsymbol{I}_q \cdot J_q \boldsymbol{I}_{-q}. \tag{4}$$

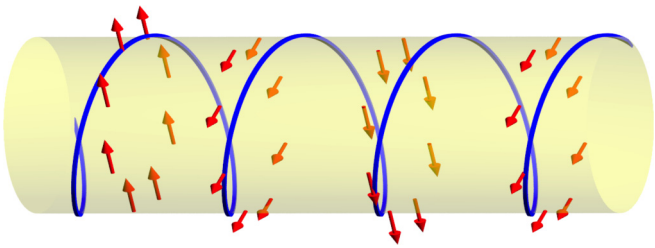

FIG. 1. (Color online) A sketch of a conducting wire (yellow cylinder) with itinerant electrons (not shown) that couple to localized nuclear spins (red arrows) via hyperfine interaction. As a result, a helical nuclear polarization emerges below a critical temperature. The blue spiral is a guide to the eye showing the direction of the helical polarization. The helical plane is chosen to be perpendicular to the wire axis (which need not be the case in general).

In one dimension, the RKKY coupling J_q has a sharp minimum at momentum $q = \pm 2k_F$, with $k_F = \sqrt{2m\varepsilon_F}/\hbar$ the electron Fermi wave vector [14,15]. Consider an approximation in which we neglect all values of J_q with respect to the large (negative) value at this minimum,

$$H_{\rm RKKY} \simeq \frac{1}{N} J_{2k_F} \left(\boldsymbol{I}_{2k_F} \cdot \boldsymbol{I}_{-2k_F} + \boldsymbol{I}_{-2k_F} \cdot \boldsymbol{I}_{2k_F} \right). \tag{5}$$

To understand the spectrum of this Hamiltonian, we introduce linearly transformed spin operators

$$\boldsymbol{I}_i = \mathcal{R}_{\boldsymbol{u}, 2k_F R_i} \hat{\boldsymbol{I}}_i, \tag{6}$$

with $\mathcal{R}_{\boldsymbol{u},\phi}$ the matrix corresponding to a rotation by angle ϕ around a unit vector $\boldsymbol{u}$. Inserting Eq. (6) into Eq. (5) we get

$$H_{\rm RKKY} \simeq \frac{1}{N} J_{2k_F} (\hat{\boldsymbol{I}}^\perp_{q=0} \cdot \hat{\boldsymbol{I}}^\perp_{q=0} + \mathcal{B}/2), \tag{7}$$

where we define the vector components along $\boldsymbol{u}$ as $\hat{I}^u = \hat{\boldsymbol{I}} \cdot \boldsymbol{u}$, and perpendicular to it as $\hat{\boldsymbol{I}}^\perp = \hat{\boldsymbol{I}} - \hat{I}^u \boldsymbol{u}$, and we separated the terms bilinear in the spin operators at finite momenta

$$\mathcal{B} = \sum_{q=\pm 2k_F} \left[2\hat{I}^u_q \hat{I}^u_{-q} + \hat{\boldsymbol{I}}^\perp_{2q} \cdot \hat{\boldsymbol{I}}^\perp_{-2q} + i\,\mathrm{sgn}(q)(\hat{\boldsymbol{I}}^\perp_{2q} \times \hat{\boldsymbol{I}}^\perp_{-2q}) \cdot \boldsymbol{u} \right]. \tag{8}$$

The first term in the bracket of Eq. (7) describes the energy of ferromagnetically coupled spins $\hat{\boldsymbol{I}}_i$: a configuration in which all these spins are collinear, along a vector perpendicular to $\boldsymbol{u}$, gives a minimal possible energy, of value $NN_\perp^2 J_{2k_F} I^2$. This configuration corresponds to a classical ground state of Eq. (4) as well, as it saturates the energy lower bound obtained using $\sum_q |\boldsymbol{I}_q|^2 = NN_\perp \sum_i |\boldsymbol{I}_i|^2$, the Parseval's identity.

Going back to the laboratory frame according to Eq. (6), the ground state corresponds to a helical configuration where the nuclear spins are oriented parallel to each other in the wire cross section, along a direction which rotates in a fixed plane as one moves along the wire with the spatial period equal to a half of the electron Fermi wavelength π/k_F (for illustration, see Fig. 1). We shall refer to this plane as the helical plane, with $\boldsymbol{u}$ being its normal unit vector. A unit vector $\boldsymbol{h} \perp \boldsymbol{u}$ gives the direction of the polarization within this plane at position $R = 0$.

Equation (7) has full spin rotation symmetry, as it is just Eq. (5) rewritten in a different reference frame. However, through the choice of the definite helicity and the vector $\boldsymbol{u}$, the first term in Eq. (7) breaks this symmetry. To restore it, the finite momenta components, Eq. (8), necessarily appear. To understand these terms in more detail, we note that choosing a frame with helicity opposite to the ground-state helicity would lead to a swap of the roles of $\hat{\boldsymbol{I}}^{\perp}_{q=0}$ and $\hat{\boldsymbol{I}}^{\perp}_{\pm 4k_F}$. Second, configurations where both helicities are populated lead to a lower energy gain. For example, choosing both with the same weight gives in the laboratory frame a spin-density wave, i.e., a cos-like oscillation along a fixed vector $\boldsymbol{I}_i = \boldsymbol{h}\cos(2k_F R_i)$, which gives only half of the energy gain of a helical order. Such oscillating, rather than rotating, configuration corresponds to the first term in Eq. (8). We therefore conclude that up to the spin rotational symmetry, which allows for arbitrary directions of $\boldsymbol{u}$, and $\hat{\boldsymbol{I}}^{\perp}$, the ground state with ferromagnetically aligned $\hat{\boldsymbol{I}}_i$ (helically ordered $\boldsymbol{I}_i$) is unique.

If the order is established, the expectation value of $\hat{\boldsymbol{I}}^{\perp}_{q=0}$ is macroscopic, and we parametrize it by a polarization p_h,

$$\langle \hat{\boldsymbol{I}}^{\perp}_{q=0} \rangle = N N_{\perp} I p_h \boldsymbol{h}, \tag{9}$$

so that $p_h = 1$ corresponds to a completely ordered state. With this, we reduce Eq. (5) by the mean field approximation to a Hamiltonian describing a set of noninteracting spins

$$H_{\mathrm{RKKY}} \simeq \sum_i \mu_N \boldsymbol{B}^N_i \cdot \boldsymbol{I}_i, \tag{10}$$

in the presence of the position-dependent internal field

$$\mu_N \boldsymbol{B}^N_i = 2 p_h N_{\perp} I J_{2k_F} \mathcal{R}_{\boldsymbol{u},2k_F R_i} \boldsymbol{h}. \tag{11}$$

This concludes a simplified derivation of the reduction of the RKKY Hamiltonian [Eq. (3)] into a set of noninteracting spins [Eq. (10)] in an effective (mean) field [Eq. (11)]. A detailed analysis of the applicability of such an approximation was given in Ref. [35], based on the derivation of the spectrum of the full Hamiltonian Eq. (3), without employing a mean field ansatz. There it was found that this approximation, in essence neglecting the long-wavelength magnons, is well justified for sub-Kelvin temperatures and wire lengths relevant for mesoscopic experiments.

As we consider the limit $A \ll \varepsilon_F$, we adopt the Bohr-Oppenheimer approximation, assuming that electrons react instantaneously to the changes in nuclear spin subsystem. Consequently, we can consider the effect of the nuclear polarization on electrons as an Overhauser field [15]

$$\mu_e \boldsymbol{B}_{Ov} = \frac{Aa}{2N_{\perp}} \sum_j \delta(r - R_j) \langle \boldsymbol{I}_j \rangle, \tag{12}$$

where μ_e is an electron magnetic moment. Thus, the electron Hamiltonian is

$$H_{el} = -\frac{\hbar^2}{2m}\partial_r^2 + \mu_e \boldsymbol{B}_{Ov} \cdot \boldsymbol{\sigma}. \tag{13}$$

In Eq. (13) we do not include electron-electron interactions explicitly. In the following, to evaluate the internal field $\boldsymbol{B}^N_i$ we use Eqs. (C4), and (C5) from Ref. [35]. In these equations electron-electron interaction is significant (for example, for the critical temperature of the helical polarization [14,15,33,35]) and therefore is included.

To describe the nuclear polarization in the wire when a bias voltage is applied, we will first investigate the behavior of one nuclear spin placed in an effective field of all others [Eq. (10)] and interacting with the bath of electrons described by Eq. (13).

III. HELICAL ELECTRONS AND FINITE VOLTAGE

To find how a nuclear spin is affected by the electrons when the bias voltage is applied, we first consider the properties of the electron bath in the wire. As already mentioned in Sec. II, the electrons are moving in the Overhauser field produced by the nuclear spins [see Eqs. (12) and (13)]. As the nuclear spins form a helix in equilibrium, this particular Overhauser field, denoted by $\boldsymbol{B}_h$, is also helical. Consequently, the electron spectrum is

$$\varepsilon_{\pm} = \frac{\hbar^2\left(k^2 + k_F^2\right)}{2m} \pm \frac{1}{m}\sqrt{m^2\mu_e^2 B_h^2 + \hbar^4 k^2 k_F^2}, \tag{14}$$

where k is the electron wave vector, and ε_- and ε_+ denote the lower and upper subbands, respectively. They are split by the gap $2\mu_e B_h$ at $k = 0$. The corresponding wave functions are

$$\Psi_{k,-}(r) = \frac{e^{ikr}}{\sqrt{L}}\left[e^{-ik_F r}\cos\frac{\theta_k}{2}\,|\uparrow\rangle + e^{ik_F r}\sin\frac{\theta_k}{2}\,|\downarrow\rangle\right], \tag{15}$$

$$\Psi_{k,+}(r) = \frac{e^{ikr}}{\sqrt{L}}\left[e^{ik_F r}\cos\frac{\theta_k}{2}\,|\downarrow\rangle - e^{-ik_F r}\sin\frac{\theta_k}{2}\,|\uparrow\rangle\right], \tag{16}$$

where $\cos\theta_k = \frac{\hbar^2 k k_F}{\sqrt{(\hbar^2 k k_F)^2 + (m\mu_e B_h)^2}}$ and $\sin\theta_k = \frac{-m\mu_e B_h}{\sqrt{(\hbar^2 k k_F)^2 + (m\mu_e B_h)^2}}$, and $|\uparrow\rangle$, $|\downarrow\rangle$ denote the spin states with spin up and spin down, respectively, where $\boldsymbol{u}$ sets the quantization axis. These expressions of the wave functions can be simplified since typically the ratio $\Lambda \equiv \mu_e B_{\max}/\varepsilon_F \ll 1$, where $B_{\max}$ is the maximum Overhauser field when all nuclei are fully polarized along a given direction. For example, for a GaAs quantum wire $\mu_e B_{\max} \simeq 68\ \mu$eV, while $\varepsilon_F \simeq 10$ meV, which gives $\Lambda \simeq 0.0068$. Consequently, we can use Λ as a small parameter.

We expand Eq. (15) in leading order of Λ, and for the states within the partial gap we get

$$\Psi_{k,-}(r) \approx \frac{1}{\sqrt{L}}\begin{cases} -e^{i(k-k_F)r}\,|\xi_R\rangle\,, & k > 0 \\ e^{i(k+k_F)r}\,|\xi_L\rangle\,, & k < 0 \end{cases} \tag{17}$$

where for right-moving electrons ($k > 0$) the spinor is $|\xi_R\rangle = |\uparrow\rangle$, and for left-moving electrons ($k < 0$) it is $|\xi_L\rangle = |\downarrow\rangle$. Therefore, within our approximation the electronic states in the partial gap are helical: the spin is determined by the propagation direction, and is opposite for left- and right-moving electrons.

Next, we consider the voltage applied to the wire and define it as the difference between the chemical potentials for the left- and right-moving electrons (see Fig. 2). Assuming a ballistic wire, the chemical potential of a given branch is constant in space. With the polarity as assumed in Fig. 2,

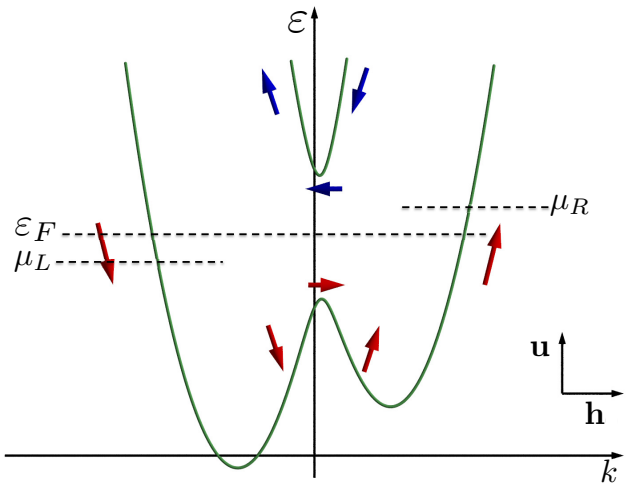

FIG. 2. (Color online) Sketch of the energy spectrum given in Eq. (18) and the direction of the electron spins in the presence of the helical Overhauser field $\boldsymbol{B}_h$ and the uniform Overhauser field $\boldsymbol{B}_u$ perpendicular to the plane of the helix. Red arrows denote the spin directions of the electrons in the lower subband, and the blue arrows label the spin directions for the upper subband. The coordinate system for the spins is formed by $\boldsymbol{h}$ and $\boldsymbol{u}$ shown in the right lower corner. The chemical potentials for left and right movers are denoted as μ_L and μ_R, respectively. The voltage applied to the wire is $eV_{RL} = \mu_R - \mu_L$.

the applied voltage depletes the left (L) branch and increases the population of the right (R) branch. This imbalance in population opens up an additional phase space for the electrons to backscatter, predominantly from R to L. Because of the helical character of the states, such backscattering is accompanied by an electron spin flip (from $|\uparrow\rangle$ to $|\downarrow\rangle$). This, in turn, is enabled by the total spin-conserving hyperfine interaction [Eq. (1)], so that each electron spin flip is compensated by a nuclear spin flip in the opposite direction. In this way, a *uniform* nuclear polarization along the $\boldsymbol{u}$ direction is built up. We denote $\boldsymbol{B}_u$ as the Overhauser field corresponding to this uniform polarization.

From Fig. 2 one can see that this scattering-induced spin polarization works only for the electronic states within the partial gap. Aiming at the helical order detection, applying voltage larger than the partial gap is therefore disadvantageous: it will not increase the spin pumping rate, but it will decrease all polarizations through heating, similarly as high temperature. We can therefore restrict our theory to small voltage, i.e., $eV < 2\mu_e B_h$, where $-e$ is the electron charge, and small temperatures T, i.e., $k_B T < 2\mu_e B_h$. We can then adopt two approximations. First, we neglect the influence from electron states which are not in the partial gap (the upper (+) subband is neglected completely), because their contribution to transport is exponentially small, proportional to $\exp[(-\mu_e B_h + eV/2)/k_B T]$. Second, we use Eq. (17) for the electron wave functions, which means that we consider Eq. (15) in leading order of $k_B T/\varepsilon_F$, eV/ε_F, and Λ. Therefore, for a description of the electron system in terms of a heat bath that causes the relaxation of the nuclear spins, we take into account two branches: left- and right-moving electrons with spins $|\downarrow\rangle$ and $|\uparrow\rangle$, respectively.

The spectrum of electrons moving in the total Overhauser field $\boldsymbol{B}_h + \boldsymbol{B}_u$ reads as

$$\varepsilon_{u,\pm} = \frac{\hbar^2\left(k^2 + k_F^2\right)}{2m} \pm \sqrt{\mu_e^2 B_h^2 + \left[\frac{\hbar^2 k k_F}{m} - \mu_e B_u\right]^2}, \quad (18)$$

see Fig. 2. The asymmetry of the spectrum is due to the uniform Overhauser field $\boldsymbol{B}_u$. The corrections to the wave functions [Eq. (17)] due to $\boldsymbol{B}_u$ are negligible in leading order of Λ. Namely, the presence of the uniform component in the Overhauser field rotates (cants) the spinors $|\xi_{L(R)}\rangle$ away from down (up) direction by a very small angle (for a maximal possible field $B_u = B_{\max}$ this angle is for our parameters smaller than 0.1°). Even though the canted up and down spinors are no longer orthogonal to each other, it does not play any substantial role. Indeed, since the spin flips of electrons are compensated by nuclei, there is no spin conservation (no selection rules) within the two subsystems taken individually.

We note that from Eqs. (15) and (16) it follows that the electron spins become also polarized, thereby producing a Knight shift acting as an effective magnetic field $\boldsymbol{B}_j^e$ back on the nuclear spins. This Knight shift is defined as $\langle H_{\rm hyp}\rangle_{el} = \mu_N \boldsymbol{B}_j^e \cdot \boldsymbol{I}_j$, where $\langle \ldots \rangle_{el}$ denotes averaging over the eigenstates of the Hamiltonian in Eq. (13) with populations defined by the voltage. In this work, however, we can neglect $\boldsymbol{B}_j^e$ with respect to $\boldsymbol{B}_j^N$ produced by the RKKY interaction [15,35].

IV. BLOCH EQUATION FOR THE TOTAL NUCLEAR SPIN IN THE WIRE

To investigate the time dynamics of the nuclear spins, we apply the standard Bloch-Redfield theory to our problem, which is valid for weak coupling between spin system and bath degrees of freedom [38,39], as is the case here. First, we write the Bloch equation for the average $\langle \boldsymbol{I}_j \rangle$ of the jth nuclear spin. By applying Eqs. (7)–(11) from Ref. [38] to our Eqs. (1), (10), and (13), we get (for more details see Appendix)

$$\partial_t \langle \boldsymbol{I}_j \rangle = \boldsymbol{\omega}_j \times \langle \boldsymbol{I}_j \rangle - \boldsymbol{\Gamma}_j \langle \boldsymbol{I}_j \rangle + \boldsymbol{\Upsilon}_j, \quad (19)$$

where $\boldsymbol{\omega}_j = \mu_N \boldsymbol{B}_j^N/\hbar$ determines the precession, the relaxation tensor $\boldsymbol{\Gamma}_j$ the decay, and the inhomogeneous vector term $\boldsymbol{\Upsilon}_j$ the stationary value of $\langle \boldsymbol{I}_j \rangle$. Both $\boldsymbol{\Gamma}_j$ and $\boldsymbol{\Upsilon}_j$ are expressed in terms of time correlators (see Appendix)

$$\mathcal{J}_{nl}(\omega) = \frac{1}{2\hbar^2}\int_0^\infty e^{-i\omega t}\langle \delta B_n(0)\delta B_l(t)\rangle_{el} dt, \quad (20)$$

where t is time, the indexes n, l label the components of the effective fluctuating internal field $\delta\boldsymbol{B}$ defined via $H_{\rm hyp} - \langle H_{\rm hyp}\rangle_{el} = \delta\boldsymbol{B}\cdot\boldsymbol{I}_j$. The time dependence follows from the interaction representation $\delta\boldsymbol{B}(t) = e^{iH_{el}t/\hbar}\delta\boldsymbol{B}e^{-iH_{el}t/\hbar}$. We note that above equations are valid for a spin $\frac{1}{2}$. However, it is well known [40] that the relaxation time of a spin into its stationary value does not depend on the spin length (in Born approximation). Thus, we will assume that our results apply for arbitrary spins.

As follows from Secs. II and III, we can define the expectation value of a nuclear spin at position $R = 0$ as

$$\langle \boldsymbol{I}_0\rangle/I = p_h \boldsymbol{h} + p_u \boldsymbol{u}, \quad (21)$$

where $0 \leqslant p_{h,u} \leqslant 1$ denote the polarizations along the two orthogonal directions $\boldsymbol{h}$ and $\boldsymbol{u}$, respectively.

We also introduce position-independent tensors $\boldsymbol{\Gamma}_0$ and $\boldsymbol{\Upsilon}_0$ in the rotated frame defined by the rotation matrix $\mathcal{R}^{\dagger}_{\boldsymbol{u},2k_F R_j}$, via

$$\boldsymbol{\Gamma}_j = \mathcal{R}_{\boldsymbol{u},2k_F R_j} \boldsymbol{\Gamma}_0 \mathcal{R}^{\dagger}_{\boldsymbol{u},2k_F R_j}, \tag{22}$$

$$\boldsymbol{\Upsilon}_j = \mathcal{R}_{\boldsymbol{u},2k_F R_j} \boldsymbol{\Upsilon}_0. \tag{23}$$

Having Eqs. (11), (19), (22), and (23), we can describe the time evolution of the nuclear spin $\boldsymbol{I}_j$ in the rotated frame.

Eventually, we are interested in the dynamics of the total (macroscopic) polarizations, rather than the one of an individual nuclear spin. We therefore introduce the total nuclear spin in the rotated frame $\sum_j \mathcal{R}^{\dagger}_{\boldsymbol{u},2k_F R_j} \langle \boldsymbol{I}_j \rangle \equiv N N_{\perp} \langle \boldsymbol{I}_0 \rangle$, and write the equation of motion for it using Eqs. (11), (19), (22), and (23). We get

$$\partial_t \langle \boldsymbol{I}_0 \rangle = -\Omega (\langle \boldsymbol{I}_0 \rangle \cdot \boldsymbol{h}) \boldsymbol{h} \times \boldsymbol{u} - \boldsymbol{\Gamma}_0 \langle \boldsymbol{I}_0 \rangle + \boldsymbol{\Upsilon}_0, \tag{24}$$

where we denoted $\Omega = I p_u |J_{2k_F}|/\hbar$. The first term implies a rotation of the helical direction $\boldsymbol{h}$, around the axis $\boldsymbol{u}$ with frequency Ω. This can be seen by introducing a time-dependent vector $\boldsymbol{h}(t) = \mathcal{R}_{\boldsymbol{u},\alpha(t)} \boldsymbol{h}$, where $\alpha(t) = \int_0^t \Omega \, d\tau$. In the Born-Oppenheimer approximation, the tensors $\boldsymbol{\Gamma}_j$ and $\boldsymbol{\Upsilon}_j$ are functions of the instantaneous values of $\boldsymbol{h}$ and $\boldsymbol{u}$, so we write

$$\tilde{\boldsymbol{\Gamma}}_j = \mathcal{R}_{\boldsymbol{u},\alpha(t)} \boldsymbol{\Gamma}_j \mathcal{R}^{\dagger}_{\boldsymbol{u},\alpha(t)}, \tag{25}$$

$$\tilde{\boldsymbol{\Upsilon}}_j = \mathcal{R}_{\boldsymbol{u},\alpha(t)} \boldsymbol{\Upsilon}_j. \tag{26}$$

With this the time evolution of $\langle \boldsymbol{I}_0 \rangle$ in the rotating frame, $\langle \tilde{\boldsymbol{I}}_0 \rangle = \mathcal{R}_{\boldsymbol{u},\alpha(t)} \langle \boldsymbol{I}_0 \rangle$, is described by

$$\partial_t \langle \tilde{\boldsymbol{I}}_0 \rangle = -\tilde{\boldsymbol{\Gamma}}_0 \langle \tilde{\boldsymbol{I}}_0 \rangle + \tilde{\boldsymbol{\Upsilon}}_0. \tag{27}$$

To evaluate the tensors in this equation, we use the results of Sec. III and approximate the electronic states within the gap by Eq. (17) and the spectrum by Eq. (18) with $B_h = 0 = B_u$. We can then use Eq. (27) to describe the polarization of the nuclear spins in the wire as function of temperature and voltage.

V. RESULTING POLARIZATIONS

To find the polarizations p_h and p_u from Eq. (27), we now evaluate the tensors $\boldsymbol{\Gamma}_0$ and $\boldsymbol{\Upsilon}_0$ explicitly. For that we first evaluate the correlator $\mathcal{J}_{nl}(\omega)$. Using Eqs. (17) and (18) we get

$$\mathcal{J}_{nl}(\omega) = \frac{A^2 a^2}{32 \hbar^3 \pi v_F^2 N_{\perp}^2} \sum_{a,b \in \{L,R\}} M_{nl}^{ab} Q_{ab}, \tag{28}$$

$$M_{nl}^{ab} = \langle \xi_a | \sigma_n | \xi_b \rangle \langle \xi_b | \sigma_l | \xi_a \rangle, \tag{29}$$

$$Q_{ab} = \int d\varepsilon \, f(\varepsilon + eV_{ba}/2) \times [1 - f(\varepsilon + \hbar\omega - eV_{ba}/2)], \tag{30}$$

where $eV_{ba} = \mu_b - \mu_a$ is the difference between chemical potentials of branches b and a, with a and b denoting L (left movers) or R (right movers). Here we also use the Fermi distribution function $f(\varepsilon) = \{\exp[\varepsilon/(k_B T)] + 1\}^{-1}$. As was mentioned in Sec. III, we consider voltages and temperatures smaller than the partial gap $2\mu_e B_h$ given by the helical polarization. Therefore, the term $f(\varepsilon + eV_{ba}/2)[1 - f(\varepsilon + \hbar\omega - eV_{ba}/2)]$ allows us to consider only the energy window of $\pm\mu_e B_h$ around ε_F because $f(\varepsilon)$ decays exponentially for $\varepsilon/k_B T \gg 1$. Consequently, we approximate the electron density of states (per spin) by $\nu(\varepsilon) \approx \nu(\varepsilon_F)$. Up to first order in Λ, we have $\nu(\varepsilon_F) = 1/(\pi \hbar v_F)$, where $v_F = \varepsilon_F/(\hbar k_F)$ is the Fermi velocity of the electrons.

Having obtained $\mathcal{J}_{nl}(\omega)$, it is straightforward to calculate $\boldsymbol{\Gamma}_0$ and $\boldsymbol{\Upsilon}_0$, using Eqs. (A2)–(A4) and (28)–(30). We can then solve Eq. (27) for the steady-state polarizations (keeping ω_0 as a constant) and obtain

$$p_h = \frac{4\hbar\omega_0}{(\hbar\omega_0 - eV)\coth\left(\frac{\hbar\omega_0 - eV}{2k_B T}\right) + (\hbar\omega_0 + eV)\coth\left(\frac{\hbar\omega_0 + eV}{2k_B T}\right) + 2\hbar\omega_0 \coth\left(\frac{\hbar\omega_0}{2k_B T}\right)}, \tag{31}$$

$$p_u = \frac{4\hbar\omega_0 \frac{(\hbar\omega_0 - eV)\coth\left(\frac{\hbar\omega_0 - eV}{2k_B T}\right) - (\hbar\omega_0 + eV)\coth\left(\frac{\hbar\omega_0 + eV}{2k_B T}\right)}{(\hbar\omega_0 - eV)\coth\left(\frac{\hbar\omega_0 - eV}{2k_B T}\right) + (\hbar\omega_0 + eV)\coth\left(\frac{\hbar\omega_0 + eV}{2k_B T}\right) + 2\hbar\omega_0 \coth\left(\frac{\hbar\omega_0}{2k_B T}\right)} + 4eV}{(\hbar\omega_0 - eV)\coth\left(\frac{\hbar\omega_0 - eV}{2k_B T}\right) + (\hbar\omega_0 + eV)\coth\left(\frac{\hbar\omega_0 + eV}{2k_B T}\right) + 2eV\coth\left(\frac{eV}{2k_B T}\right)}. \tag{32}$$

However, from Eq. (11) it follows that $\hbar\boldsymbol{\omega}_0 = 2p_h N_{\perp} I J_{2k_F} \boldsymbol{h}$, i.e., ω_0 depends on p_h. This leads to nonlinear algebraic equations for two unknowns p_u and p_h, which we solve numerically using material parameters for GaAs (analytical expressions for small deviations of the polarizations are given in the following). We plot the values obtained in this way and discuss their behavior as a function of voltage and temperature, the experimental parameters that are most directly accessible.

The voltage dependence of the polarizations is shown in Fig. 3. We can see that the polarization p_u grows faster with voltage than p_h decays, therefore, the overall polarization of the nuclei $\sqrt{p_u^2 + p_h^2}$ grows with voltage, too. This means that the nuclear spins are more polarized when a voltage is applied than when they are in equilibrium at the same temperature. We also note that having a nonzero component p_u means that nuclear spins have a conical polarization, rather than a helical one. To plot Fig. 3, we used Eqs. (C4) and (C5) from Ref. [35] as was mentioned above, where the dependence of $\hbar\omega_0$ on temperature is described in detail. To evaluate $\hbar\omega_0$ we used the characteristic values for GaAs: the Fermi velocity $v_F = 2.3 \times 10^5$ m/s, and the number of nuclei in the wire cross section

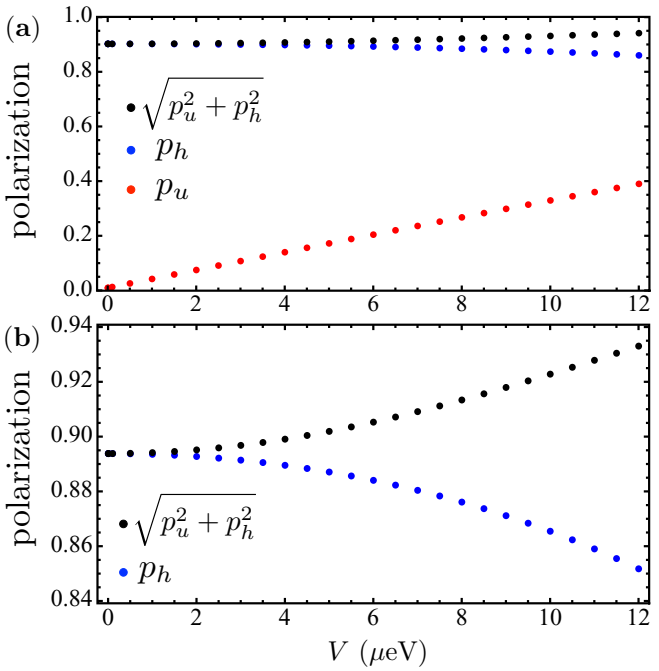

FIG. 3. (Color online) (a) The voltage dependence of the polarization p_h along helical direction $\boldsymbol{h}$ (blue), polarization p_u in the direction of $\boldsymbol{u}$ perpendicular to the helix plane (red), and the overall polarization of nuclei $\sqrt{p_u^2+p_h^2}$ (black). (b) Enlarged from (a) the voltage dependence of p_h and $\sqrt{p_u^2+p_h^2}$. We use $T = 90$ mK and other parameters as given in the text. We recall that our parametrization is such that $p_u = 1$ corresponds to $B_u = B_{\max}$, which is about 5 T in GaAs, and analogously for B_h.

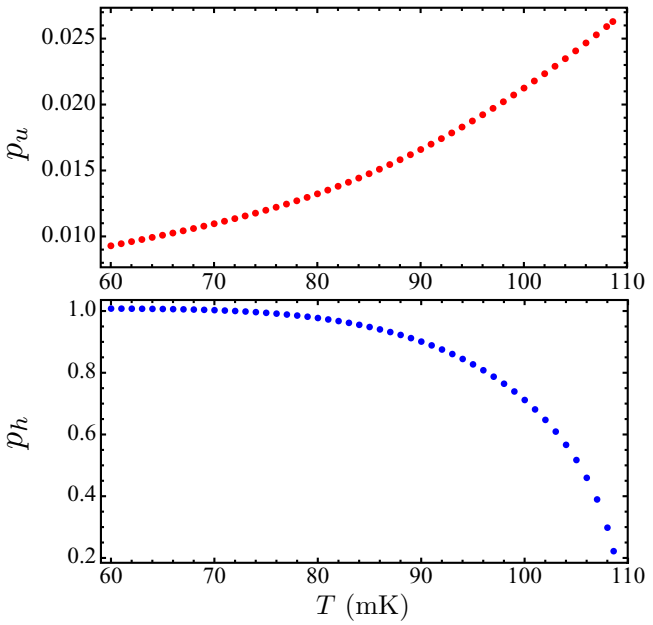

FIG. 4. (Color online) Plot of the temperature dependence of the polarization p_u (upper panel, red) and the polarization p_h (lower panel, blue). For these plots the same parameters were used as in Fig. 3 and the applied voltage is $eV = 0.5$ μeV. We note that our calculation is valid for $eV, k_B T < 2\mu_e B_h$, therefore the smallest value of p_h we consider here is $p_h \simeq 0.2$.

$N_\perp = 1300$. For the expression for J_{2k_F} taken from Ref. [35] we use the electron-electron interaction Luttinger liquid parameter $K_\rho = 0.2$ and the absolute value of spin $I = \frac{3}{2}$. For the constants described above and at $T = 90$ mK and $p_u = 0.1$ the rotation frequency of the nuclear spin helix is $\Omega \approx 1.5 \times 10^6$ s^{-1}.

It is natural to expect that high temperature destroys the nuclear helical order [14,15,33,35]. Indeed, Fig. 4 shows that the helical polarization p_h decays with temperature and then drops in magnitude around $T \simeq 109$ mK. As our calculation is valid for $eV, k_B T < 2\mu_e B_h$, the smallest value of p_h allowed by self-consistency for our parameters is $p_h \simeq 0.2$. From Fig. 4 it also follows that the polarization p_u grows with temperature. This growth is explained by the fact that due to higher temperature, the electron states with higher energy become occupied. This makes the nuclear spin flip more probable. It is obvious that there is a temperature where the polarization p_u gets destroyed, however, for the range of temperatures given in Fig. 4, p_u does grow, whereas the helical polarization p_h decays significantly. The decay of p_h with temperature is rapid, while the growth of p_u is less pronounced. Therefore, the overall nuclear polarization in the wire strongly decays with increasing temperature. For the parameters we used for Fig. 4 the effect of temperature on p_h is stronger than the one of a finite voltage. The initial temperature scaling of p_h away from unity (see Fig. 4) can be obtained readily from Eq. (31) by treating $1 - p_h$ as a small perturbation. This yields

$$p_h \approx 1 - \frac{2}{1+e^{\frac{\kappa}{Tg}}} \frac{1}{1-\frac{\kappa}{2Tg}\operatorname{sech}^2\left(\frac{\kappa}{2Tg}\right)} \tag{33}$$

$$\approx 1 - 2e^{-\frac{\kappa}{Tg}}, \tag{34}$$

where the first equality holds well for the temperature interval 60 mK $< T <$ 90 mK, while the second one is a good approximation for 60 mK $< T <$ 80 mK. Here we denoted $g = 3 - \frac{4K_\rho}{\sqrt{2(1+K_\rho^2)}}$, and the temperature-independent parameter $\kappa = 2N_\perp I |J_{2k_F}| T^{g-1}/k_B$ depends on the material and geometrical properties of the sample (see Eq. (11) and Eqs. (C4) and (C5) of Ref. [35]). For $K_\rho = 0.2$ (chosen for the plots) we get $g = 2.4$ (we recall that $K_\rho = g = 1$ corresponds to vanishing electron-electron interactions).

The initial decrease of p_h due to voltage in Fig. 3 for $V <$ 3 μeV scales as

$$p_h \approx \alpha - \gamma V^2, \tag{35}$$

where α and γ depend on material and geometrical parameters of the nanowire and on temperature.

Finally, we mention that recent progress in nuclear spin magnetometry on nanowires [36,37] has opened the perspective to measure the nuclear spin polarizations directly and thus to test the predictions made here. Moreover, due to the helical nuclear polarization which acts on electrons as an Overhauser field $\boldsymbol{B}_h$ there is a partial gap in the electron spectrum [see Eq. (18)]. As a result, the conductance of a ballistic nanowire is less than $2e^2/h$ for sufficiently low temperatures and $V < 2\mu_e B_h$ [14,15,32,35]. As was shown

above, the polarization p_h, and consequently $\boldsymbol{B}_h$, decrease with increasing voltage and temperature. We thus expect qualitatively that the conductance of the wire will increase with the decrease of the partial gap $2\mu_e B_h \propto p_h$ [41].

VI. CONCLUSIONS

We have shown that due to the hyperfine interaction between electrons and nuclei in the wire the applied voltage changes the form of the nuclear polarization and its amplitude. Assuming that in equilibrium there is a helical nuclear polarization p_h present in the wire due to RKKY interaction, a bias voltage induces a uniform polarization p_u perpendicular to the helix plane. Due to this polarization, the nuclear spin helix starts to rotate around the axis perpendicular to the helical plane. When a nonzero polarization p_u builds up, the nuclear polarization changes from helical to conical.

We have also presented the voltage dependence of p_u and p_h and seen that p_u increases with voltage, whereas p_h decreases. Following from these two effects the overall nuclear polarization in the wire grows with voltage. Remarkably, p_u grows with temperature in the considered range of temperatures. This is because the nuclear spin flip becomes more probable as electrons occupy higher energy states. This thermal activation effect is noticeable for the considered regime $\hbar\omega_0 > eV$. The growth of the overall polarization $\sqrt{p_u^2 + p_h^2}$ with voltage and the growth of p_u with temperature are intriguing and *a priori* nonobvious effects. The polarization effects predicted here might be observed in transport experiments [32] or more directly via cantilever-based nanoscale magnetometry [36,37].

Finally, we note that the current-induced dynamical effects we found are not restricted to nuclear helimagnets. Among other systems, they are expected to appear in a wire with magnetic impurities, such as Mn-doped GaAs, once the helical order in the impurities is RKKY-induced. Even for moderate dopings, in such a system the coupling constant A/ρ_0, which is central to the energy scales in question, is more than 1000 times larger than for nuclear spins. Even though the critical temperature can not be directly estimated from this ratio, as it is strongly influenced also by the electron-electron interactions, it is still expected to be larger by several orders of magnitudes compared to the sub-Kelvin range typical for nuclear spins. Although this was not our focus here, we note that, correspondingly, the partial gap and the resulting upper bound on the applied voltage will move to mV scale, more realistic for possible spintronics device applications.

ACKNOWLEDGMENTS

We thank V. N. Golovach, D. Becker, B. Braunecker, L. Glazman, C. Kloeffel, T. Meng, and C. Orth for helpful discussions and acknowledge support from the Swiss NF, NCCR QSIT, and S^{3}NANO.

APPENDIX: BLOCH EQUATION FOR ONE NUCLEAR SPIN

To write the Bloch equation for the total nuclear spin in the wire, we use Eqs. (7)– (11) from Ref. [38]. Here we present them adopted to our case of a nuclear spin interacting with the bath of electrons and placed into the effective field produced by all other nuclear spins in the wire.

The Bloch equation for the nth nuclear spin reads as

$$\partial_t \langle \boldsymbol{I}_n \rangle = \boldsymbol{\omega}_n \times \langle \boldsymbol{I}_n \rangle - \boldsymbol{\Gamma}_n \langle \boldsymbol{I}_n \rangle + \boldsymbol{\Upsilon}_n. \tag{A1}$$

To express tensors $\boldsymbol{\Gamma}_n$ and $\boldsymbol{\Upsilon}_n$ we introduce a unit vector $\boldsymbol{l}$ along $\boldsymbol{\omega}_n$, i.e., $\boldsymbol{\omega}_n = \omega_n \boldsymbol{l}$. The tensor $\boldsymbol{\Gamma}_n$ consists of a dephasing part $\boldsymbol{\Gamma}_n^d$ which comes from energy-conserving processes and a pure relaxation part $\boldsymbol{\Gamma}_n^r$, which comes from the energy exchange with the bath [38,42] (played here by the electron system)

$$\boldsymbol{\Gamma}^d_{n,ij} = \delta_{ij} l_p l_q \mathcal{J}^+_{pq}(0) - l_i l_p \mathcal{J}^+_{pj}(0), \tag{A2}$$

$$\begin{aligned}\boldsymbol{\Gamma}^r_{n,ij} = {} & \delta_{ij}(\delta_{pq} - l_p l_q)\mathcal{J}^+_{pq}(\omega_n) - (\delta_{ip} - l_i l_p)\mathcal{J}^+_{pj}(\omega_n) \\ & - \delta_{ij}\epsilon_{kpq} l_k \mathcal{I}^-_{pq}(\omega_n) + \epsilon_{ipq} l_p \mathcal{I}^-_{qj}(\omega_n).\end{aligned} \tag{A3}$$

Here, the indexes i, j denote components of tensors, and we use the Einstein convention of summation over repeated indexes. Further, ϵ_{pqk} is the Levi-Civita symbol and δ_{ij} the Kronecker delta, while l_k denotes the kth component of vector $\boldsymbol{l}$. The inhomogeneous part of the Bloch equation $\boldsymbol{\Upsilon}_n$ reads as [38,42]

$$\begin{aligned}\boldsymbol{\Upsilon}_{n,i} = {} & \tfrac{1}{2}\{l_j \mathcal{J}^-_{ij}(\omega_n) - l_i \mathcal{J}^-_{jj}(\omega_n) + \epsilon_{ipq}\mathcal{I}^+_{pq}(\omega_n) \\ & + \epsilon_{iqk} l_k l_p [\mathcal{I}^+_{pq}(\omega_n) - \mathcal{I}^+_{pq}(0)]\},\end{aligned} \tag{A4}$$

where i denotes the component of $\boldsymbol{\Upsilon}_n$. The terms $\mathcal{J}^{\pm}_{ij}(\omega)$, $\mathcal{I}^{\pm}_{ij}(\omega)$ are defined as

$$\mathcal{J}^{\pm}_{ij}(\omega) = \mathrm{Re}[\mathcal{J}_{ij}(\omega) \pm \mathcal{J}_{ij}(-\omega)], \tag{A5}$$

$$\mathcal{I}^{\pm}_{ij}(\omega) = \mathrm{Im}[\mathcal{J}_{ij}(\omega) \pm \mathcal{J}_{ij}(-\omega)]. \tag{A6}$$

The term $\mathcal{J}_{ij}(\omega)$ is the Laplace transformation of the correlator of the fluctuating fields $\delta\boldsymbol{B}$ at different times

$$\mathcal{J}_{ij}(\omega) = \frac{1}{2\hbar^2}\int_0^\infty e^{-i\omega t}\langle \delta B_i(0)\delta B_j(t)\rangle_{el} dt, \tag{A7}$$

where $\delta\boldsymbol{B}(t) = e^{iH_{el}t/\hbar}\delta\boldsymbol{B}e^{-iH_{el}t/\hbar}$. Using Eq. (A1), we expressed the Bloch equation for the total nuclear spin in the wire resulting in Eq. (24).

[1] S. S. P. Parkin, M. Hayashi, and L. Thomas, Science **320**, 190 (2008).
[2] D. Rugar, H. J. Mamin, M. H. Sherwood, M. Kim, C. T. Rettner, K. Ohno, and D. D. Awschalom, Nat. Nanotechnol. **10**, 120 (2015).
[3] C. Kloeffel and D. Loss, Annu. Rev. Condens. Matter Phys. **4**, 51 (2013).
[4] H. Fröhlich and F. R. N. Nabarro, Proc. R. Soc. London, Ser. A **175**, 382 (1940).
[5] M. A. Ruderman and C. Kittel, Phys. Rev. **96**, 99 (1954).

[6] T. Kasuya, Prog. Theor. Phys. **16**, 45 (1956).
[7] K. Yosida, Phys. Rev. **106**, 893 (1957).
[8] T. Dietl, A. Haury, and Y. M. d'Aubigné, Phys. Rev. B **55**, R3347 (1997).
[9] H. Ohno, Science **281**, 951 (1998).
[10] P. Simon and D. Loss, Phys. Rev. Lett. **98**, 156401 (2007).
[11] P. Simon, B. Braunecker, and D. Loss, Phys. Rev. B **77**, 045108 (2008).
[12] H. Ohno, D. Chiba, F. Matsukura, T. Omiya, E. Abe, T. Dietl, Y. Ohno, and K. Ohtani, Nature (London) **408**, 944 (2000).
[13] D. Chiba, M. Sawicki, Y. Nishitani, Y. Nakatani, F. Matsukura, and H. Ohno, Nature (London) **455**, 515 (2008).
[14] B. Braunecker, P. Simon, and D. Loss, Phys. Rev. Lett. **102**, 116403 (2009).
[15] B. Braunecker, P. Simon, and D. Loss, Phys. Rev. B **80**, 165119 (2009).
[16] D. C. Dixon, K. R. Wald, P. L. McEuen, and M. R. Melloch, Phys. Rev. B **56**, 4743 (1997).
[17] T. Machida, S. Ishizuka, T. Yamazaki, S. Komiyama, K. Muraki, and Y. Hirayama, Phys. Rev. B **65**, 233304 (2002).
[18] E. V. Deviatov, A. Würtz, A. Lorke, M. Yu. Melnikov, V. T. Dolgopolov, D. Reuter, and A. D. Wieck, Phys. Rev. B **69**, 115330 (2004).
[19] C. J. Trowbridge, B. M. Norman, Y. K. Kato, D. D. Awschalom, and V. Sih, Phys. Rev. B **90**, 085122 (2014).
[20] K. Chida, M. Hashisaka, Y. Yamauchi, S. Nakamura, T. Arakawa, T. Machida, K. Kobayashi, and T. Ono, Phys. Rev. B **85**, 041309(R) (2012).
[21] S. Chesi and W. A. Coish, arXiv:1503.03645.
[22] J. C. Slonczewski, J. Magn. Magn. Mater. **159**, L1 (1996).
[23] L. Berger, Phys. Rev. B **54**, 9353 (1996).
[24] G. Tatara, H. Kohno, and J. Shibata, Phys. Rep. **468**, 213 (2008).
[25] F. Li, T. Nattermann, and V. L. Pokrovsky, Phys. Rev. Lett. **108**, 107203 (2012).
[26] K. M. D. Hals and A. Brataas, Phys. Rev. B **87**, 174409 (2013).
[27] J. C. Budich, F. Dolcini, P. Recher, and B. Trauzettel, Phys. Rev. Lett. **108**, 086602 (2012).
[28] J. Maciejko, C. Liu, Y. Oreg, X.-L. Qi, C. Wu, and S.-C. Zhang, Phys. Rev. Lett. **102**, 256803 (2009).
[29] T. L. Schmidt, S. Rachel, F. von Oppen, and L. I. Glazman, Phys. Rev. Lett. **108**, 156402 (2012).
[30] A. M. Lunde and G. Platero, Phys. Rev. B **86**, 035112 (2012).
[31] A. Del Maestro, T. Hyart, and B. Rosenow, Phys. Rev. B **87**, 165440 (2013).
[32] C. P. Scheller, T.-M. Liu, G. Barak, A. Yacoby, L. N. Pfeiffer, K. W. West, and D. M. Zumbühl, Phys. Rev. Lett. **112**, 066801 (2014).
[33] P. Stano and D. Loss, Phys. Rev. B **90**, 195312 (2014).
[34] A. A. Zyuzin, T. Meng, V. Kornich, and D. Loss, Phys. Rev. B **90**, 195125 (2014).
[35] T. Meng, P. Stano, J. Klinovaja, and D. Loss, Eur. Phys. J. B **87**, 203 (2014).
[36] P. Peddibhotla, F. Xue, H. I. T. Hauge, S. Assali, E. P. A. M. Bakkers, and M. Poggio, Nat. Phys. **9**, 631 (2013).
[37] B. E. Herzog, D. Cadeddu, F. Xue, P. Peddibhotla, and M. Poggio, Appl. Phys. Lett. **105**, 043112 (2014).
[38] V. N. Golovach, A. Khaetskii, and D. Loss, Phys. Rev. Lett. **93**, 016601 (2004).
[39] K. Blum, *Density Matrix Theory and Applications*, 2nd ed. (Plenum, New York, 1996).
[40] C. P. Slichter, *Principles of Magnetic Resonance* (Springer, Berlin, 1980).
[41] However, we caution that the behavior of the polarizations $p_{h,u}$ can only indicate the trend for the conductance but does not give its precise dependence on temperature and voltage. Indeed, in transport new temperature and voltage effects emerge, especially in the transition region where the partial gap is comparable to temperature and voltage.
[42] M. Borhani, V. N. Golovach, and D. Loss, Phys. Rev. B **73**, 155311 (2006).